

This is the Accepted Manuscript version of an article accepted for publication in Nanotechnology. IOP Publishing Ltd is not responsible for any errors or omissions in this version of the manuscript or any version derived from it. The Version of Record is available online at [DOI: 10.1088/1361-6528/ab2aad].

Fine printing method of silver nanowires electrodes with alignment and accumulation

Ashuya Takemoto^{1,2,3}, Teppei Araki^{1,2,3}, Yuki Noda¹, Takafumi Uemura^{1,3},
Shusuke Yoshimoto¹, Robert Abbel⁴, Corne Rentrop⁴, Jeroen van den Brand⁴ and
Tsuyoshi Sekitani^{1,2,3,a)}

¹The Institute of Scientific and Industrial Research, Osaka University, Ibaraki, [567-0047], Japan

²Department of Applied Physics, Graduate School of Engineering, Osaka University, Suita, [565-0871], Japan

³Advanced Photonics and Biosensing Open Innovation Laboratory, AIST-Osaka University, Suita, [565-0871], Japan

⁴Holst Centre, Eindhoven, [5656 AE], the Netherlands

E-mail: sekitani@sanken.osaka-u.ac.jp

Received xxxxxx

Accepted for publication xxxxxx

Published xxxxxx

Abstract

One-dimensional metal nanowires offer great potential in printing transparent electrodes for next-generation optoelectronic devices such as flexible displays and flexible solar cells. Printing fine patterns of metal nanowires with widths $< 100 \mu\text{m}$ is critical for their practical use in the devices. However, the fine printing of metal nanowires onto polymer substrates remains a major challenge owing to their unintended alignment. This paper reports on a fine-printing method for transparent silver nanowires (AgNWs) electrodes miniaturized to a width of $50 \mu\text{m}$ on ultrathin ($1 \mu\text{m}$) polymer substrate, giving a high yield of $> 90\%$. In this method, the AgNW dispersion, which is swept by a glass rod, is spontaneously deposited to the hydrophilic areas patterned on a hydrophobic-coated substrate. The alignment and accumulation of AgNWs at the pattern periphery are enhanced by employing a high sweeping rate of $> 3.2 \text{ mm/s}$, improving electrical conductivity and pattern definition. The more aligned and more accumulated AgNWs lower the sheet resistance by a factor of up to 6.8. In addition, a high pattern accuracy $\leq 3.6 \mu\text{m}$, which is the deviation from the pattern designs, is achieved. Quantitative analyses are implemented on the nanowire alignment to understand the nanowire geometry. This fine-printing method of the AgNW electrodes will provide great opportunities for realizing flexible and high-performance optoelectronic devices.

Keywords: printed electronics, silver nanowires, alignment, transparent electrodes

1. Introduction

Transparent electrodes that are conventionally made of indium tin oxide (ITO) play an important role in optoelectronic devices such as displays and solar cells. Recently, as the emerging replacements to ITO, carbon nanotubes (CNT) [1, 2], graphene [3–5], conductive polymers [6, 7], and metal

nanowires [8–10] have attracted considerable attention for next-generation optoelectronic devices such as flexible displays and flexible solar cells owing to their solution processability and mechanical flexibility. In particular, silver nanowire (AgNW) electrodes have exhibited excellent performance in a high optical transmittance of $> 90\%$ [11], low sheet resistance of $< 20 \Omega/\text{sq}$ [12], and mechanical

flexibility with $> 100\%$ strain [13]. The simultaneous achievements of transparency, low resistance, and excellent mechanical flexibility and durability have not yet been realized on other materials, so far. Thus, AgNWs electrodes have been intensively explored for wearable electronics and flexible fiber electronics [14–16].

Realizing fine patterns of AgNWs with $< 100\ \mu\text{m}$ width is critical for their practical use in the pixels and grid patterns of flexible displays and capacitive touch panels. However, the conventional fine-patterning methods with photolithography [17] or laser ablation [18] would easily cause disconnections between nanowires, leading to a loss of conductivity with high material consumption. Furthermore, there exists a difficulty in implementing these methods on flexible polymer substrates because of the use of harsh solvents or high-energy sources. In contrast, additive manufacturing (i.e., printing methods) is an attractive alternative because the potential cost effectiveness is independent of the required pattern resolution [19]. Thus, ink jet printing [20], screen printing [21], and gravure printing [22] for AgNWs electrodes have been suggested. However, among these printing methods, hurdles in fine patterning exist owing to unintended bleeding or dewetting of ink [23]. To address these hurdles, Yang et al. [24] have utilized hydrophilic microchannels surrounded by a hydrophobic layer for the fine patterning of AgNWs. However, the fine patterning has not yet been realized onto polymer substrates because the hydrophilic microchannel needs to be created by photolithography process on a rigid silicon wafer. Because of these hurdles, the fine patterning of AgNWs electrodes with additive techniques on a polymer substrate is still challenging.

Herein, we propose a fine-printing method for transparent AgNWs electrodes, which enables a pattern width down to $50\ \mu\text{m}$ on an ultrathin polymer substrate. In this method, the AgNW dispersion, which is swept by a glass rod, is spontaneously deposited to the hydrophilic areas patterned on a hydrophobic-coated substrate. An yield for AgNWs electrodes was obtained as $> 90\%$. The more aligned and more accumulated AgNWs were formed at the pattern periphery by employing a high sweeping rate of $> 3.2\ \text{mm/s}$, improving the electrical conductivity and the pattern definition. The nanowire alignment was quantitatively studied using the image analysis techniques. The developed method will pave the way for printing high-performance transparent electrodes on flexible polymer substrates with low material consumption.

2. Experimental

2.1 Hydrophobic/Hydrophilic-patterned surface

The hydrophobic/hydrophilic-patterned surface was prepared as follows. First, the hydrophobic surface was fabricated by spin coating a fluorocarbon agent (WP-100; Daikin Industries, Ltd., Osaka, JPN) on a $1\text{-}\mu\text{m}$ -thick poly(para-xylylene)

polymer film (dix-SR; Daisankasei Co., Ltd., Ichihara, JPN) supported on a glass substrate (Eagle XG; Corning Inc., Corning, NY, USA). The substrate size was $2\ \text{cm} \times 3\ \text{cm}$. Then, hydrophilic areas were selectively introduced by exposing the hydrophobic surface to vacuum-ultraviolet (VUV) light through a photomask. This VUV exposure was conducted for 15 s using a radiofrequency discharge lamp (Flat Excimer EX-mini; Hamamatsu Photonics K.K., Shizuoka, JPN) with a distance of $\sim 10\ \text{mm}$ between the lamp and the hydrophobic surface.

After the VUV exposure of the hydrophobic surface, the measurement results of X-ray photoelectron spectroscopy (XPS, JSP-9010MX; JEOL, Akishima, JPN) indicated the disappearance of the F1s orbital from the hydrophobic surface. In addition, the surface profiler (DektakXT DXT-A; Bruker Corp., Billerica, MA, USA) detected an ablated thickness of less than 10 nm. These results indicate the removal of the hydrophobic coating. This removal was also confirmed by measuring the contact angles (DM-500; Kyowa Interface Science Co., Ltd., Saitama, JPN). The contact angles of the AgNW dispersion decreased from $\sim 52^\circ$ to $\sim 26^\circ$ after VUV

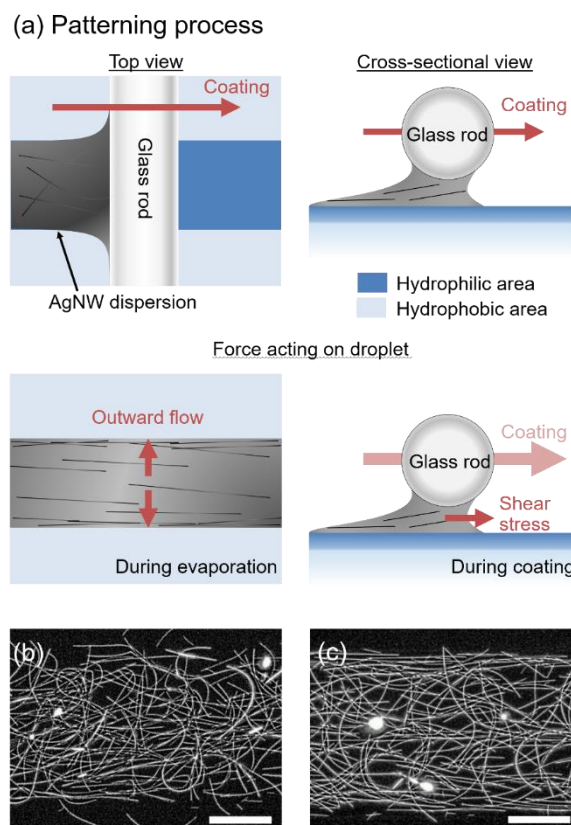


Figure 1. (a) Schematic illustrations of patterning process with hydrophobic/hydrophilic-patterned areas for fabricating electrodes on a $1\text{-}\mu\text{m}$ -thick polymer substrate. Dark-field optical images of $50\text{-}\mu\text{m}$ -wide AgNW electrodes coated at (b) low sweeping rate ($0.4\ \text{mm/s}$) and (c) high sweeping rate ($3.6\ \text{mm/s}$). The scale bar represents $20\ \mu\text{m}$.

exposure. The dispersion comprises isopropyl alcohol ~50%, water ~30%, ethanol ~15%, methanol ~5%, and AgNWs ~0.15%. The viscosity is estimated to 1–3 cP with the reference [25] and the composition of the solution. In a reference test, the contact angles of distilled water also decreased from ~110° to ~89°. Hence, the VUV exposure with a photomask yielded hydrophilic patterns on the hydrophobic surface.

2.2 AgNWs electrodes

For fine patterning of the AgNW electrodes, 1-mm-long straight hydrophilic patterns with widths of 50–250 μm were prepared with the aforementioned process. The AgNW dispersion employed in this study had AgNWs with average width and length of 39 nm and 13 μm , respectively (Showa Denko K.K., Tokyo, JPN). We used a glass rod to sweep 20 μL of the AgNW dispersion over the hydrophobic/hydrophilic-patterned surface at a distance of ~250 μm from the substrate surface to the rod bottom. The glass rod employed is commercially available and is generally used to mix chemicals and liquids in laboratories. The nature of the glass rod is hydrophilic such that the dispersion spreads along the glass rod from edge to edge on the substrate even if

the substrate is hydrophobic. The substrate was kept at room temperature (approximately 20°C) in the sweeping process. The sweeping rate was controlled by a custom-made system with a stepping motor. The dispersion preferentially wetted the hydrophilic areas, forming AgNW-based electrodes. The samples were heated for 1 h at 120 °C in near-vacuum (approximately 100 Pa). The AgNW electrodes were observed under a dark field with an optical microscope (DM4000 M; Leica Microsystems, Wetzlar, DEU). The electrical sheet resistance was measured via two-point measurement (U1252B; Keysight Technologies, Santa Rosa, CA, USA) with silver pads deposited on the AgNW electrodes.

3. Result and Discussion

Fig. 1(a) shows a schematic of the patterning process. The AgNW dispersion was swept over the prepared substrate in the longitudinal direction of the hydrophilic patterns. Due to the differences in surface energy, the AgNW dispersion was spontaneously deposited on the hydrophilic areas [24, 26]. In this process, the dispersion was possibly subjected to shear stress [24, 27] during rod coating or to outward flux [28] during drying (Fig. 1(a)). The former can preferentially enhance the nanowire alignment to the sweeping direction [24,

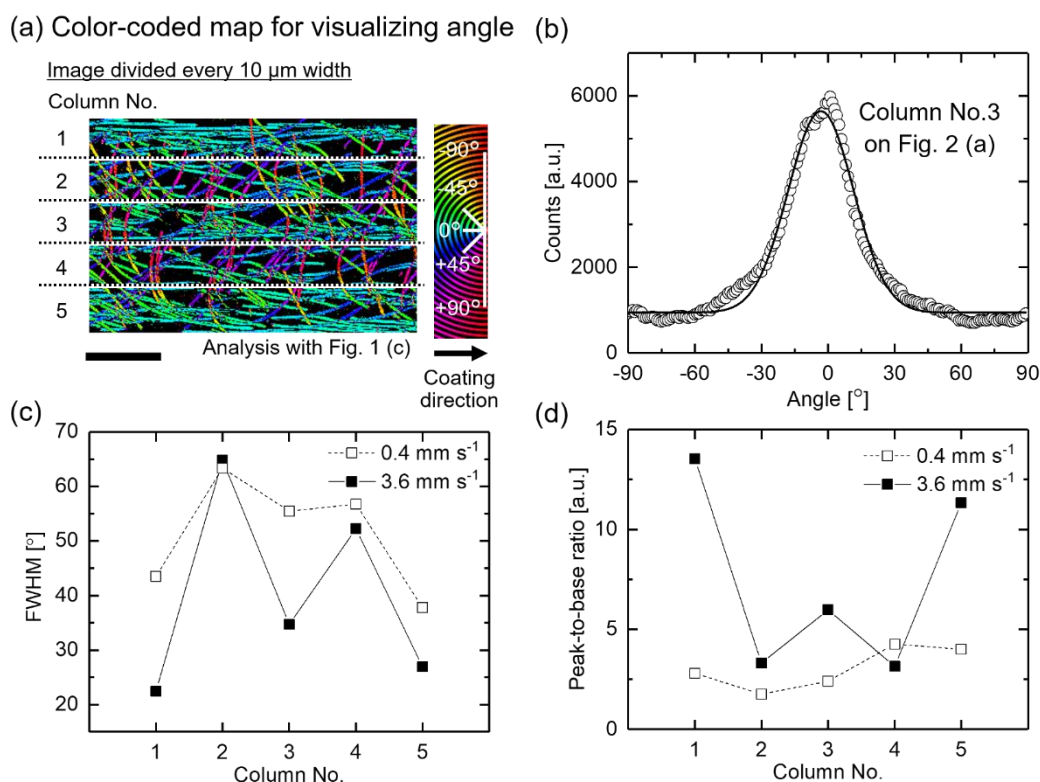


Figure 2. Nanowire alignment in the AgNW electrodes patterned on a hydrophilic area with a width of 50 μm . (a) Color-coded map indicating the local angle of nanowires on segments of the image in Fig. 1(c). The scale bar represents 20 μm . The segmentation was done in five zones with a periphery (column Nos. 1, 5) and an interior (column Nos. 2–4). (b) Angular distribution of column No. 3 from Fig. 2(a), relative to the coating direction. (c) FWHM and (d) P/B for each segmented area of AgNW electrodes patterned at sweeping rates of 0.4 and 3.6 mm/s .

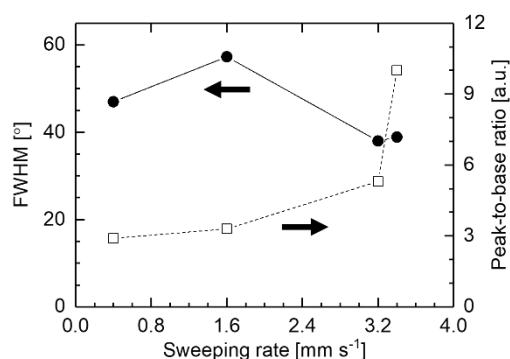


Figure 3. FWHM (filled circles) and P/B (open squares) for AgNW electrodes patterned at various sweeping rates of 0.4–3.6 mm/s for the analysis of the whole area of the 50- μ m-wide electrode.

27]. The latter, known as the coffee-stain effect [28], can cause the nanowires to drift towards the periphery. Fig. 1(b) shows the 50- μ m-wide AgNW electrode prepared at a sweeping rate of 0.4 mm/s, forming a relatively random nanowire network with unclear edges. In contrast, at a higher sweeping rate of 3.6 mm/s, the nanowire alignment at the periphery was clearly enhanced (Fig. 1(c)).

Surface tension and surface free energy determine the wettability, which was evaluated as a fundamental factor in the context of developing spontaneous deposition of the AgNW dispersion. The surface free energy of the hydrophobic and hydrophilic surfaces and the surface tension of the AgNWs dispersion were determined using the Owens–Wendt–Kaelble equation [29] with the measured contact angles and the previously reported surface tensions [30, 31]. For this calculation, we used the parameters of distilled water, ethylene glycol, and isopropyl alcohol. The measured contact angles on the hydrophobic and hydrophilic surfaces are $\sim 110^\circ$ and $\sim 89^\circ$ for water, $\sim 85^\circ$ and $\sim 75^\circ$ for ethylene glycol, and $\sim 40^\circ$ and $\sim 8^\circ$ for isopropyl alcohol, respectively. With these values and the surface tensions from the literatures [30, 31], the surface free energy of the hydrophobic and hydrophilic surfaces were obtained as 20.1 ± 0.6 mN/m and 25.4 ± 1.3 mN/m, respectively, while the surface tension of the AgNWs dispersion was 23.4 ± 4.2 mN/m. This result implies that the AgNW dispersion meets the basic requirement to wet the hydrophilic surface, and can support the fine deposition of the AgNWs under control of the sweeping rates, as shown in Fig. 1.

To study network geometry of the printed AgNWs, we investigated the nanowire alignment using the optical image of Fig. 1(c) and OrientationJ [32], a plug-in for ImageJ. Fig. 2(a) shows a color-coded image indicating the local orientation angles of the nanowires with respect to the coating direction. The image was segmented into the periphery

(column Nos. 1 and 5) and the interior (column Nos. 2–4) for comparisons between the areas. To quantitatively describe the nanowire alignment, we obtained the angular distribution from each image (column Nos. 1–5) and fitted a Gaussian function. As a typical case, Fig. 2(b) shows the fitting curve with the angular distribution of column 3 for a sweeping rate of 0.4 mm/s. The fitting curve was used to extract two parameters: the full width at half maximum (FWHM) and the peak-to-base ratio (P/B) [24]. A lower FWHM and a higher P/B indicate that the nanowires exhibit greater alignment to the sweeping direction.

Fig. 2(c) shows the FWHMs of column Nos. 1–5 for the AgNW electrodes patterned with sweeping rates of 0.4 and 3.6 mm/s. At the periphery (column Nos. 1 and 5), the sweeping rate of 3.6 mm/s results in FWHMs 1.4–2.0 times lower than those from a sweeping rate of 0.4 mm/s. In addition, the sweeping rate of 3.6 mm/s results in high P/Bs of 11–14 at the periphery, which are 3–4 times higher than those from a sweeping rate of 0.4 mm/s (Fig. 2(d)). These results indicate that the higher sweeping rate (i.e., 3.6 mm/s) produced greater alignment (i.e., lower FWHM and higher P/B) of AgNWs at the periphery. In contrast, for column Nos. 2–4, for both sweeping rates, the FWHMs are relatively high and the P/Bs are relatively low, which means the alignment is not remarkably high in the interior—the best alignment was observed in column No. 3 at a sweeping rate of 3.6 mm/s, with a relatively low FWHM ($\sim 35^\circ$) and a relatively high P/B (~ 6), but the alignment is not as high as at the periphery. The alignment analyses with the segmented images show that the higher sweeping rate improved the alignment of AgNW networks at the periphery with relatively random alignment in the interior (Figs. 2(c), (d)).

Such different network geometries on a single pattern can be attributed to the outward flux of the dispersion during drying [28]. In this study, the drying process of the AgNW dispersion on the hydrophilic-patterned areas was visually monitored with unaided eyes at different sweeping rates. Whereas the dispersion was still wet for several seconds after sweeping at the rate of 3.6 mm/s, it had immediately dried at the sweeping rate of 0.4 mm/s. This suggests that the higher sweeping rate of 3.6 mm/s ensures more volume deposition and longer drying time, resulting in the outward flux [28], which could enhance nanowire alignment at the periphery.

For the further insight, we investigated the relationship between the sweeping rate and the nanowire alignment over the entirety of a single pattern. Fig. 3 shows the FWHMs and the P/Bs of the AgNWs in the 50- μ m-wide patterns prepared with different sweeping rates (0.4–3.6 mm/s). As the sweeping rate was increased, the FWHM decrease from 47° to 38° . Concurrently, the P/B increased monotonically from 3 to 10. At a sweeping rate of 3.6 mm/s, the P/Bs were 2 times higher than those for sweeping rates of 3.2 mm/s and below, which might be due to the shear stress [24, 27]. This was therefore

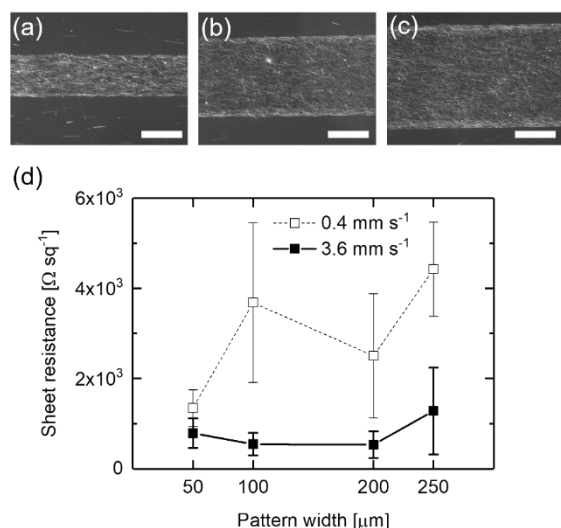


Figure 4. Observation and characterization of patterned AgNW electrodes. Dark field optical images of samples with widths of (a) 100 μm , (b) 200 μm , and (c) 250 μm for electrodes fabricated at a sweeping rate of 3.6 mm/s. The scale bar represents 100 μm . (d) Sheet resistance of AgNW electrodes patterned at sweeping rates of 0.4 and 3.6 mm/s as a function of the pattern width. At least 11 samples were measured and the average values and standard deviations are plotted.

the cause of the higher alignment degree obtained in each segmented image by employing the higher sweeping rate (Fig. 2(c) and (d)).

The highly-aligned nanowires at the periphery can be introduced to patterning AgNWs with various widths. Figs. 4(a)–(c) show AgNW electrodes patterned with different widths by coating at the same rate of 3.6 mm/s. All electrodes show a higher density of highly-aligned AgNWs at the periphery (FWHM of $< 44^\circ$ and P/B of > 8). Wang et al. [33] reported that larger droplets of the AgNW dispersion enhance the coffee-stain effect. Similarly, we observed stronger coffee-stain effects on the wider patterns (Fig. 4(a)–(c)). This accumulation of highly-aligned nanowires at the periphery improved the line definition compared to the samples patterned with the lower sweeping rate of 0.4 mm/s. When the AgNW dispersion was swept at the higher rate, the deviation of the actual patterned widths from the mask design dimensions was smaller (3.6 μm and 6.1 μm for sweeping rates of 3.6 mm/s and 0.4 mm/s, respectively). In addition, the electrical sheet resistance in the coating direction was also improved for 1-mm-long AgNW electrodes with widths of 50–250 μm (Fig. 4(d)). Yields of the electrodes prepared with both sweeping rates (3.6 and 0.4 mm/s) were obtained as $> 90\%$: at least 11 conductive electrodes for total 12 samples. The average sheet resistances for electrodes patterned with the higher sweeping rate of 3.6 mm/s were in the range of 537–1284 Ω/sq , which are 1.7–6.8 times lower than those patterned at 0.4 mm/s. This improvement in electrical characteristics

should be attributed to the higher AgNW density at the periphery of the electrodes [34]. On comparison, these values of sheet resistance are higher than the state-of-the-art AgNWs electrodes with a few tens Ω/sq [27, 35–39]. However, the fine-printed AgNWs electrodes were only subjected to heating at 120°C after coating. We found out that the resistance can be reduced into 3–93% (Average: 53%) of the initial resistance with thermal annealing at 200°C for 10 min by preparing large-area AgNWs conductive films of 2 cm \times 2 cm. In the future, other techniques [15] such as plasmonic welding, electrochemical coating, and mechanical pressing might be also effective for further reduction in resistance of the fine-printed electrodes.

To estimate the optical transparency, we extracted the fractional area coverage of nanowires on a single pattern prepared with the higher sweeping rate (3.6 mm/s) by using the optical images and ImageJ. The estimated coverage on patterns with widths of 50–250 μm was approximately 30–40%, which means the transmittance at $\lambda = 550 \text{ nm}$ could be estimated as $> 70\%$ from the previous report of Bergin et al. [35]. For this estimation, we referred to the relationship between the area fraction and transmittance of the AgNWs with approximately same lengths and width as the ones we used. The high estimated transmittance was attributed to the lower AgNW density in the center. In addition, the actual optical transmittance might be higher than this estimated value, because the observed size of the nanowires should be larger than the actual size owing to the observation of their scattering light.

4. Conclusion

In conclusion, we have demonstrated the rod-coating technique with the hydrophobic/hydrophilic- patterned surface, resulting in fine-printed AgNW transparent electrodes with aligned and accumulated nanowires along the pattern periphery. The alignment analyses indicate that strong alignment can be formed at the periphery of the patterns by employing a higher sweeping rate. Such patterns of AgNW transparent electrodes experienced improved sheet resistance and patterning accuracy. In the recent reports [27, 36–39], alignment technology of the AgNWs has been explored for coating the entire surfaces of the substrates without patterning. However, alignment of nanowires should be implemented together with fine patterning for the practical use of printed AgNWs electrodes in flexible optoelectronics. In these terms, the fine printability on ultrathin polymer substrates and the alignment improvement on the fine patterns, simultaneously, have been demonstrated in this work. Furthermore, the patterning method we have developed can be used to create two different functionalities, i.e., dense and sparse networks, on a single electrode with widths down to 50 μm . This approach will provide great opportunities for realizing high-

performance optoelectronic devices with transparent fine-printed AgNW electrodes.

Acknowledgements

We thank the following collaborators for the useful discussions and equipment applications: Prof. K. Sugauma and Prof. M. Nogi of the ISIR, the Comprehensive Analysis Center in ISIR, Showa Denko K. K., and Guy Bex of Holst Centre. This work was partially supported by JSPS KAKENHI Grant Number JP17K17866, the Center of Innovation Program from JST, and the JSPS Core-to-Core Program.

Author Contributions

A.T. and T.A. equally contributed and performed the project. A.T., T.A., Y.N., S.Y., T.U. and T.S. designed the patterning experiments and the electrical measurements. R.A., C.R. and J.v.d.B. contributed to the image analyses.

References

- [1] Wu Z, Chen Z, Du X, Logan J M, Sippel J, Nikolou M, Kamaras K, Reynolds J R, Tanner D B, Hebard A F and Rinzler A G 2004 transparent, conductive carbon nanotube films *Science* **305** 1273
- [2] Lipomi D J, Vosgueritchian M, Tee B C-K, Hellstrom S L, Lee J A, Fox C H and Bao Z 2011 Skin-like pressure and strain sensors based on transparent elastic films of carbon nanotubes *Nat. Nanotechnol.* **6** 788
- [3] Eda G, Fanchini G and Chhowalla M 2008 Large-area ultrathin films of reduced graphene oxide as a transparent and flexible electronic material *Nat. Nanotechnol.* **3** 270
- [4] Kim K S, Zhao Y, Jang H, Lee S Y, Kim J M, Kim K S, Ahn J-H, Kim P, Choi J-Y and Hong B H 2009 Large-scale pattern growth of graphene films for stretchable transparent electrodes *Nature* **457** 706
- [5] Bae S, Kim H, Lee Y, Xu X, Park J-S, Zheng Y, Balakrishnan J, Lei T, Ri Kim H, Song Y Il, Kim Y-J, Kim K S, Özyilmaz B, Ahn J-H, Hong B H and Iijima S 2010 Roll-to-roll production of 30-inch graphene films for transparent electrodes *Nat. Nanotechnol.* **5** 574
- [6] Kim Y H, Sachse C, Machala M L, May C, Müller-Meskamp L and Leo K 2011 Highly Conductive PEDOT:PSS electrode with optimized solvent and thermal post-treatment for ITO-free organic solar cells *Adv. Funct. Mater.* **21** 1076–81
- [7] Vosgueritchian M, Lipomi D J and Bao Z 2012 Highly conductive and transparent PEDOT:PSS films with a fluorosurfactant for stretchable and flexible transparent electrodes *Adv. Funct. Mater.* **22** 421–28
- [8] Lee J-Y, Connor S T, Cui Y and Peumans P 2008 Solution-processed metal nanowire mesh transparent electrodes *Nano Lett.* **8** 689–92
- [9] Hu L, Kim H S, Lee J-Y, Peumans P and Cui Y 2010 Scalable coating and properties of transparent, flexible, silver nanowire electrodes, *ACS Nano* **4** 2955–63
- [10] Madaria A R, Kumar A and Zhou C 2011 Large scale, highly conductive and patterned transparent films of silver nanowires on arbitrary substrates and their application in touch screens *Nanotechnology* **22** 245201
- [11] Moon H., Won P, Lee J and Ko S H 2016 Low-haze, annealing-free, very long Ag nanowire synthesis and its application in a flexible transparent touch panel, *Nanotechnology* **27** 295201
- [12] Liang J, Li L, Niu X, Yu Z and Pei Q 2013 Elastomeric polymer light-emitting devices and displays, *Nat. Photonics* **7** 817–24
- [13] Yang Y, Ding S, Araki T, Jiu J, Sugahara T, Wang J, Vanfleteren J, Sekitani T and Sugauma K 2016 Facile fabrication of stretchable Ag nanowire/polyurethane electrodes using high intensity pulsed light *Nano Research* **9** 401–14
- [14] Zeng W, Shu L, Li Q, Chen S, Wang F and Tao X M 2014 Fiber-based wearable electronics: A review of materials, fabrication, devices, and applications *Adv. Mater.* **26** 5310–36
- [15] Sannicolo T, Lagrange M, Cabos A, Celle C, Simonato J -P and Bellet D 2016 Metallic nanowire-based transparent electrodes for next generation flexible devices: a review *Small* **12** 6052–75
- [16] Yan W, Page A, Nguyen-Dang T, Qu Y, Sordo F, Wei L and Sorin F 2019 Advanced multimaterial electronic and optoelectronic fibers and textiles, *Adv. Mater.* **31** 1802348
- [17] Ahn Y, Lee H, Lee D and Lee Y 2014 Highly conductive and flexible silver nanowire-based microelectrodes on biocompatible hydrogel *ACS Appl. Mater. Interfaces* **6** 18401–7
- [18] Hong S, Yeo J, Lee J, Lee H, Lee P, Lee S S and Ko S H 2015 Selective laser direct patterning of silver nanowire percolation network transparent conductor for capacitive touch panel, *J. Nanosci. Nanotechnol.* **15** 2317–23
- [19] Li D, Lai W-Y, Zhang Y-Z and Huang W 2018 Printable transparent conductive films for flexible electronics *Adv. Mater.* **30** 1704738
- [20] D. J. Finn, M. Lotya and J. N. Coleman, *ACS Appl. Mater. Interfaces* **7**, 9254 (2015). Finn D J, Lotya M and Coleman J N 2015 Inkjet printing of silver nanowire networks *ACS Appl. Mater. Interfaces* **7** 9254–61
- [21] Liang J, Tong K and Pei Q 2016 A water-based silver-nanowire screen-print ink for the fabrication of stretchable conductors and wearable thin-film transistors, *Adv. Mater.* **28** 5986–96
- [22] Park J D, Lim S and Kim H 2015 Patterned silver nanowires using the gravure printing process for flexible applications, *Thin Solid Films* **586** 70–5
- [23] Matsui H, Noda Y and Hasegawa T 2012 Hybrid energy-minimization simulation of equilibrium droplet shapes on hydrophilic/hydrophobic patterned surfaces *Langmuir* **28** 15450–3
- [24] Yang B -R, Cao W, Liu G -S, Chen H -J, Noh Y -Y, Minari T, Hsiao H -C, Lee C -Y, Shieh H -P D and Liu C 2015 Microchannel wetting for controllable patterning and alignment of silver nanowire with high resolution *ACS Appl. Mater. Interfaces* **7** 21433–41
- [25] Wensink E J W, Hoffmann A C, Van Maaren P J and Van Der Spoel D 2003 Dynamic properties of water/alcohol mixtures studied by computer simulation *J. Chem. Phys.* **119** 7308–17
- [26] Liu X, Kanehara M, Liu C, Sakamoto K, Yasuda T, Takeya J and Minari T 2016 Spontaneous patterning of high-resolution

- electronics via parallel vacuum ultraviolet *Adv. Mater.* **28** 6568–73
- [27] Cho S, Kang S, Pandya A, Shanker R, Khan Z, Lee Y, Park J, Craig S L and Ko H 2017 Large-area cross-aligned silver nanowire electrodes for flexible, transparent, and force-sensitive mechanochromic touch screens *ACS Nano* **11** 4346–57
- [28] Deegan R D, Bakajin O, Dupont T F, Huber G, Nagel S R and Witten T A 1997 Capillary flow as the cause of ring stains from dried liquid drops *Nature* **389** 827–9
- [29] Kwok D Y and Neumann A W 1999 Contact angle measurement and contact angle interpretation *Adv. Colloid Interface Sci.* **81** 167–249
- [30] Jańczuk B, Białopiotrowicz T and Wójcik W 1989 The surface tension components of aqueous alcohol solutions *Colloids Surf.* **36** 391–403
- [31] Shimizu R N and Demarquette N R 2000 Evaluation of surface energy of solid polymers using different models *J. Appl. Polym. Sci.* **76** 1831–45
- [32] Rezakhanliha R, Agianniotis A, Schrauwen J T C, Griffa A, Sage D, Bouten C V C, van de Vosse F N, Unser M and Stergiopoulos N 2012 Experimental investigation of collagen waviness and orientation in the arterial adventitia using confocal laser scanning microscopy *Biomech. Model. Mechanobiol.* **11** 461–73
- [33] Wang X, Kang G, Seong B, Chae I, Yudistira H T, Lee H, Kim H and Byun D 2017 Transparent arrays of silver nanowire rings driven by evaporation of sessile droplets *J. Phys. D Appl. Phys.* **50** 455302
- [34] Shimoni A, Azoubel S and Magdassi S 2014 Inkjet printing of flexible high-performance carbon nanotube transparent conductive films by “coffee ring effect” *Nanoscale* **6** 11084–9
- [35] Bergin S M, Chen Y -H, Rathmell A R, Charbonneau P, Li Z -Y and Wiley B J 2012 The effect of nanowire length and diameter on the properties of transparent, conducting nanowire films *Nanoscale* **4** 1996–2004
- [36] Kang S, Kim T, Cho S, Lee Y, Choe A, Walker B, Ko S -J, Kim J Y and Ko H 2015 Capillary printing of highly aligned silver nanowire transparent electrodes for high-performance optoelectronic devices *Nano Lett.* **15** 7933–42
- [37] Hu H, Pauly M, Felix O and Decher G 2017 Spray-assisted alignment of layer-by-layer assembled silver nanowires: a general approach for the preparation of highly anisotropic nanocomposite films. *Nanoscale* **9** 1307–14
- [38] Dong J and Goldthorpe I A 2018 Exploiting both optical and electrical anisotropy in nanowire electrodes for higher transparency *Nanotechnology* **29** 045705
- [39] Meng L, Bian R, Guo C, Xu B, Liu H and Jiang L 2018 Aligning Ag nanowires by a facile bioinspired directional liquid transfer: toward anisotropic flexible conductive electrodes *Adv. Mater.* **30** 1706938